Partially Overlapping NOMA System with Many Neighboring Channels

Zoltán Belső, László Pap

***Abstract*—The increasing usage of the Internet of Things (IoT) and other modern massive machine-type communication applications has led to a growing demand for more efficient u tilization o f a vailable c ommunication bandwidth. These applications necessitate the concurrent operation of multiple communication channels. The classical approach is Orthogonal Multiple Access (OMA), such as Time Division Multiple Access (TDMA) or Frequency Division Multiple Access (FDMA). However, an emerging alternative is Non-Orthogonal Multiple Access (NOMA), where communicating parties share one or more resources. The power domain NOMA scheme employs superposition coding (SC) and successive interference cancellation (SIC) to mitigate the effects of interference caused by overlapping frequency bands. Our proposal presents a partial NOMA solution: we retain the bandwidth division from the FDMA scheme but allow for partial overlap between neighboring channels. In this approach, we do not apply SIC; instead, we treat the interference caused by the overlap as part of the noise. This scheme enables the use of a wider bandwidth for individual channels. By carefully controlling the extent of overlap, we achieve a capacity increase resulting from the wider bandwidth that outweighs the capacity loss due to increased noise.**

***Index Terms*—NOMA, non-orthogonal, multiple access, FDMA.**

I. Introduction

Many modern applications, including the Internet of Things (IoT) and other massive machine-type communication applications, require multiple communication channels with similar characteristics to operate simultaneously. The available resources, such as bandwidth and transmit power, are always limited and must be shared among these channels.

In the classical Orthogonal Multiple Access (OMA) scheme, one or more of these resources are divided between the channels to prevent interference between the signals of different channels. Two commonly used OMA schemes are Time Division Multiple Access (TDMA) and Frequency Division Multiple Access (FDMA). In TDMA, only one channel is allowed to communicate at a time, enabling that channel to utilize the full available bandwidth and transmit power. In FDMA, the bandwidth is divided into smaller pieces, with each channel using its designated piece of the spectrum continuously [1]. Both of these schemes have practical limitations that result in some portion of the divided resources being wasted. In TDMA, the transition from one user to another cannot occur instantaneously; a certain guard time is required, during which no communication takes place. Similarly in FDMA, the channels cannot be placed closely adjacent to each other. Each subchannel's spectral characteristics have finite roll-off, requiring a wider bandwidth than the Nyquist bandwidth (see figure 1). In this paper, we will focus on FDMA to make more efficient use of the available bandwidth. An emerging alternative is Non-Orthogonal Multiple Access (NOMA), where communicating parties share one or more of these resources in a non-orthogonal manner. One of the most discussed methods is Power Domain NOMA [2], [3], [4], [5]. This method is based on superposition coding (SC), where the signals of all simultaneous users are added (superimposed onto each other).

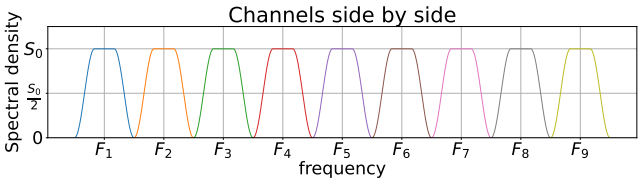

Fig. 1. Channels in FDMA with finite roll-off

In the case of uplink communication, where many clients communicate with a single base station, all the clients transmit simultaneously, utilizing the full bandwidth. In the case of downlink communication, where a single base station transmits to many clients simultaneously, all the users' signals are added together and transmitted, utilizing the entire bandwidth.

On the receiver side, the superimposed signals are decoded one by one, with the interference from other signals treated as part of the noise. The strongest signal is decoded first, even if it's not intended for the given client. After successfully demodulating the signal, the receiver remodulates it and subtracts the result from the received signal, thereby eliminating the interference caused by that signal. Then it can demodulate the next strongest signal. Then it proceeds to demodulate the next strongest signal. By continuing this successive process, the receiver can eventually reach the signal intended for it. This technique is known as successive interference cancellation.

Manuscript received January 31, 2024; revised April 29, 2024. Date of publication July 30, 2024. Date of current version July 30, 2024. The associate editor prof. Joško Radić has been coordinating the review of this manuscript and approved it for publication.

Authors are with the Department of Networked Systems and Services, Budapest University of Technology and Economics, 1117, Budapest, Magyar tudósok krt. 2., Hungary (e-mails: {belso,pap}@hit.bme.hu).

Digital Object Identifier (DOI): 10.24138/jcomss-2024-0002

The NOMA method offers advantages over the OMA method in terms of achievable channel capacity in both uplink and downlink scenarios. The extent of this advantage depends on the channel conditions of the participating channels. NOMA provides greater benefits when there are significant differences in the channels' signal-to-noise ratio (SNR) conditions. In the corner case where all the channels have the same SNR, the achievable capacity region remains the same for both NOMA and OMA [3], [4].

The successive interference cancellation (SIC) process necessitates precise channel estimation since remodulation must accurately replicate the channel's effect, including both amplitude gain and phase shift, on the transmitted signal. Any inaccuracies in channel estimation result in performance degradation due to imperfect cancellation. Numerous papers have explored channel estimation in various scenarios [6], [7]. This degradation becomes more pronounced as the difference between the SNR conditions of the participating users increases. Interestingly, this is the very scenario where NOMA stands to benefit the most over OMA. However, the advantage could diminish due to imperfect channel estimation.

NOMA with SIC was considered as a study item in 3GPP for 5G New Radio (NR); however, it was dropped and left for possible use beyond 5G. One of the reasons behind dropping the study item was the implementation complexity, especially receiver complexity [8]. In our proposed method, we consider classical FDMA without utilizing SIC. We investigate how to increase spectral efficiency and thus channel capacity without increasing receiver complexity using partial NOMA technique.

Our proposal is a kind of in-between solution. While NOMA channels fully overlap, FDMA channels have no overlap at all. Our approach suggests allowing a partial overlap between neighboring channels, without employing SIC, thus eliminating the need for precise channel estimation and receiver complexity. Instead, the interference caused by the overlap is treated as noise during demodulation.

By permitting a slight overlap between neighboring channels, we aim to reduce the bandwidth loss resulting from finite roll-off channel filter characteristics. This allows for the expansion (stretching) of individual channel bandwidths, resulting in increased channel capacity that can potentially offset the capacity loss due to increased noise.

There is a trade-off here to consider: excessive stretching can lead to a significant increase in noise, while insufficient stretching may result in diminishing capacity gains. Our goal is to investigate the optimal stretching factor in this context.

In [9], the authors suggest a similar approach but from the opposite direction: it retains SIC but slightly reduces the full overlap of power domain NOMA to enhance the capacity of the far downlink station (the one that cannot cancel the interference). The authors find that a slight reduction in overlap can be beneficial, increasing the sum of the achievable bitrate.

In [10], the authors propose partial-NOMA in a large two-user downlink network to provide both throughput and reliability. For signal decoding, the authors propose a complicated technique called flexible successive interference cancellation (FSIC). In their model, they consider a downlink cellular network where the base stations are distributed according to a homogeneous Poisson point process, and they consider only two users. Their goal is to maximize the cell sum rate given a threshold minimum throughput constraint.

In a recent conference paper [11], the authors propose a partial NOMA solution for a semi-integrated sensing and communication system. This involves simultaneous communication signal from infrastructure-to-vehicle (I2V) and sensing signal from vehicle-to-vehicle (V2V). The authors suggest a partial overlap between these two signals.

In Orthogonal Frequency Division Multiplexing (OFDM) systems, the frequency band is divided into subchannels in a special way, such that the signals of the individual subchannels overlap, yet the signals are still orthogonal. OFDM systems have some challenges to overcome. In order to maintain orthogonality in the system, all components, including all the power amplifiers must be linear. Due to the fact that the baseband signal is a composition of many sinusoidal signals with different phases, the peak-to-average power ratio (PAPR) is low, which poses a challenge to the power amplifier. Many solutions have been proposed to increase the PAPR of OFDM systems. Recently, applying NOMA technique to address these problems is gaining popularity. In [12], the authors propose a special precoding matrix to be applied in order to increase PAPR. Another study in the field is [13], where the authors analyze the effect of the nonlinear distortion causing non-orthogonality in the signal.

Our approach is different from these proposals mainly in that we propose having overlap without employing SIC. Only a slight overlap can be beneficial in this case, but all the complexity and dependence on precise channel estimation of the power domain NOMA system are eliminated this way. Our proposal can also be seen as an extension of the classical FDMA OMA system by introducing slight non-orthogonality, thereby improving the spectral inefficiency of the FDMA system originating from having finite roll-off channel filter characteristics.

In [14] we have already investigated this approach for the most basic case of spectral shape. The authors only considered one user stretching its bandwidth to gain capacity but did not investigate the effect on the neighbors. The authors find that capacity can be gained but do not investigate the optimal stretching factor. In this paper, we consider a more realistic spectral shape, the root raised cosine. We consider many channels side by side and apply stretch to all of them. That means, for any given channel, interference is coming from both sides. We calculate the capacity gain as a function of the stretching factor and find the optimal stretching in different SNR environments.

Our main contributions are as follows:

- We show that by widening the bandwidth of the individual channels in a multi-channel communication system without changing the channel spacing, we can achieve higher spectral efficiency and increase the bitrate achievable by all the channels opposed to traditional OMA FDMA systems, without increasing receiver complexity.
- We propose not to employ SIC so that the complexity of the receivers can be reduced, and the dependency on

precise channel estimation can be eliminated compared to classical power domain NOMA systems.
- We calculate the effect of the interference caused by spectral overlap. We show that there is an optimal level of channel bandwidth stretching depending on the channel conditions (SNR values) and the channel filter characteristic (roll-off factor) employed. The derived formulas are general and can be applied in any combination of neighboring channel conditions.
- We calculate the optimal stretching and the achievable capacity gain as a function of the channel condition (SNR) and filter characteristic (roll-off factor) for some practically important cases.

This paper is structured as follows: First, we formalize the basic model, including channel filter parameters. Next, we calculate the excess noise caused by interference. Subsequently, we evaluate the system capacity and determine the optimal stretching factor across various system parameters. Finally, we summarize our findings.

II. Basic Model: Partially Overlapping Channels

The capacity (or achievable bit rate) of a communication channel (C) with a given power (P) and bandwidth (W) is [15], [16]:

$$C = W \cdot \log_2\left(1 + \frac{P}{N_0 \cdot W}\right) = W \cdot \log_2\left(1 + SNR\right) \quad (1)$$

where SNR denotes the signal to noise ratio, and N_0 is the spectral power density of the ever present background noise. The total noise power entering the receiver is $N = N_0 W$ so the SNR is:

$$SNR = \frac{P}{N_0 \cdot W} \quad (2)$$

In this paper, we consider a system with many channels placed side by side. This is a common situation in a massive machine-type communication applications that utilize a frequency division multiple access (FDMA) scheme. In an orthogonal multiple access (OMA) system, the channels occupied by neighboring users do not overlap (see figure 1). However, due to the practical limitations of transmit and receive filters in real systems, there exists a transition range at both edges of the channel.

A. Root Raised Cosine Filter

In our analysis, we consider the commonly used filter characteristic known as root raised cosine [17]. Figure 2. illustrates two neighboring channels, but it's important to note that there are many such channels, and the same pattern repeats on both sides.

Since we are considering numerous independent communication channels with similar purposes, we assume that these channels share the same parameters. Specifically, the power spectral density ($S_{0_1} = S_{0_2} = S_0$), the signaling time ($T_{s_1} = T_{s_2} = T_s$) and the roll-off factor ($\alpha_1 = \alpha_2 = \alpha$) are identical. This assumption is not crucial for our calculations; the derived results are general and can be applied in cases where the neighboring channels have different characteristics.

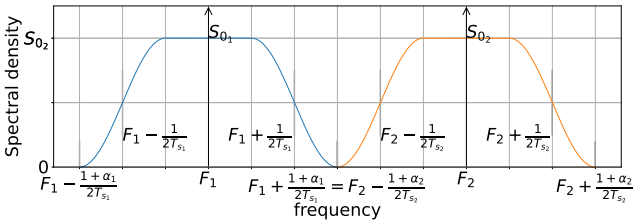

Fig. 2. Two adjacent channels without overlap

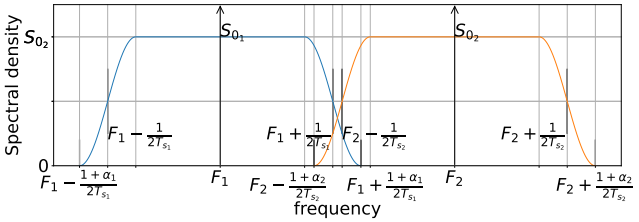

Fig. 3. Two adjacent channels with overlap

The formulation of such a signal spectral density around the center frequency (F) is:

$$X(f) = \begin{cases} S_0 & |f| \le \frac{1-\alpha}{2T_s} \\ \frac{S_0}{2}\{1+ & \\ +\cos\left[\frac{\pi T_s}{\alpha}\left(|f| - \frac{1-\alpha}{2T_s}\right)\right]\} & \frac{1-\alpha}{2T_s} \le |f| \le \frac{1+\alpha}{2T_s} \\ 0 & |f| \ge \frac{1+\alpha}{2T_s} \end{cases} \quad (3)$$

The channels are occupying a bandwidth of

$$W_{occ} = \frac{1+\alpha}{T_s} \quad (4)$$

which is greater than the Nyquist bandwidth:

$$W = \frac{1}{T_s} \quad (5)$$

The larger the α parameter, the wider the occupied bandwidth becomes. In certain segments where the spectral response rolls off, the spectral density of the signal is lower than the maximum density (S_0). However, due to the symmetrical nature of the raised cosine characteristic, the total power of the signal is given by:

$$P = \int_{-\infty}^{\infty} S(f)df = \int_{F+\frac{1+\alpha}{2T_s}}^{F-\frac{1+\alpha}{2T_s}} S(f)df = W \cdot S_0 \quad (6)$$

Since the noise entering the receiver is also shaped by the same receive filter, the total noise power remains $N = W \cdot N_0$.

B. Bandwidth Stretching

The concept involves enhancing bandwidth utilization by permitting partial overlap between neighboring channels. The model is that we keep the same spacing between the channels, keeping the center frequencies (F_1 and F_2) unchanged. However, the approach expands the occupied bandwidth of an individual channel by reducing the signaling period ($T_s' < T_s$),

and increasing the Nyquist bandwidth ($W' = \frac{1}{T'_S} > W$). Please refer to figure 3. for a spectral representation of this scenario. This expansion or stretching of bandwidth can be quantified by the stretching factor, denoted as x:

$$x = \frac{W'}{W} = \frac{T_s}{T'_s} \tag{7}$$

In our model, the total transmit power (P) remains constant, so the power spectral density ($S'_0 < S_0$) decreases:

$$P = W \cdot S_0 = W' \cdot S'_0 = \frac{S'_0}{T'_s} \tag{8}$$

or what is equivalent:

$$P = \frac{S_0}{T_s} = \frac{S'_0}{T'_s} \tag{9}$$

Therefore, we can represent the new spectral density level as:

$$S'_0 = S_0 \frac{T'_s}{T_s} = \frac{S_0}{x} \tag{10}$$

III. Interference as Extra Noise

In our model, we consider the modulation content of neighboring channels to be independent. This implies that the partially overlapping signals from neighboring channels are uncorrelated. The overlapping portion of the interfering signal can be treated as if it were independent random Gaussian noise. As outlined in [18] and [19] such interference can be modeled by introducing an equivalent additional spectral noise power density, N'_0, added to the ever present background noise spectral density N_0.

A. The Extra Noise Power Density

The level of the extra noise power density is expressed as [18]:

$$N'_0 = \frac{\int_{-\infty}^{\infty} S'_1(f - F_1) S'_2(f - F_2) df}{\int_{-\infty}^{\infty} S'_1(f - F_1) df} \tag{11}$$

where $S'_1(f)$ is the spectral density function of the channel of interest (after bandwidth stretching), and $S'_2(f)$ represents the spectral density of the interfering neighboring channel. In our model, all channels share the same characteristics, and they all apply the same bandwidth stretching. Therefore, both $S'_1(f)$ and $S'_2(f)$ are described by (3) with parameters α and T'_s.

Please note that the denominator in (11) corresponds to the total power of the signal of interest, as defined in (6). Additionally, observe that the integrand in the numerator is non-zero only in regions where $S'_1(f)$ is non-zero. Therefore, we can eliminate the improper integral, simplifying N'_0 as follows:

$$N'_0 = \frac{\int_{F_1 - \frac{1+\alpha}{2T'_s}}^{F_1 + \frac{1+\alpha}{2T'_s}} S'_1(f - F_1) S'_2(f - F_2) df}{P} \tag{12}$$

This extra noise power density is then added to the background noise (N_0) as:

$$N_0 + N'_0 = N_0 \left(1 + \frac{N'_0}{N_0}\right) \tag{13}$$

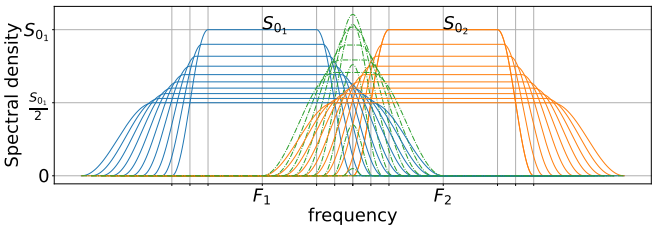

Fig. 4. The first channel is stretched between a factor of 1 and 2. The dotted line is the product of the two spectral density function.

It's worth noting that in the classical OMA case, where there is no overlap between $S_1(f)$ and $S_2(f)$, the integrand is zero, and thus $N'_0 = 0$.

In figure 4, we observe two neighboring channels with varying degrees of overlap. The stretching factor (x) defined in (7) ranges from 1 (indicating no stretching and no overlap) to 2 (resulting in a doubling of the occupied bandwidth). In accordance with our model, we assume that both channels undergo the same degree of stretching. Given that these channels share identical parameters, such as signaling rate and roll-off factor, a scenario with $x = 2$ signifies that the overlap extends up to the center frequency of each channel.

Furthermore, following our model, we consider the presence of multiple channels placed side by side, all undergoing the same stretching process. Hence, there is another channel on the opposite side as well (for the sake of clarity, not depicted in figure 4.). When $x = 2$, this implies that the channel overlap from the other side also extends to the center frequency. Any further stretching would lead to the overlapping of three channels. Up to this point, we can treat the interference from the two neighboring channels as independent, simply summing the extra noise power emanating from both sides.

B. Normalized Spectral Density

In the following discussion, we employ the same derivation as presented in [14] to express the extra noise power N'_0 using normalized spectral densities, denoted as:

$$S^n(f) = \frac{S(f)}{P} \tag{14}$$

This normalization ensures that:

$$\int_{-\infty}^{\infty} S^n(f) df = 1 \tag{15}$$

Hence, N'_0 can be expressed as:

$$N'_0 = P \int_{-\infty}^{\infty} S_1^{n\prime}(f - F_1) S_2^{n\prime}(f - F_2) df \tag{16}$$

Here, $S_1^{n\prime}$ and $S_2^{n\prime}$ represent the normalized spectral densities of the two overlapping channels. Although we will later assume them to be equal, for the sake of clarity and generality, we keep them distinct for the time being.

Denoting the value of the integral as:

$$N^e = \int_{-\infty}^{\infty} S_1^{n\prime}(f - F_1) S_2^{n\prime}(f - F_2) df \tag{17}$$

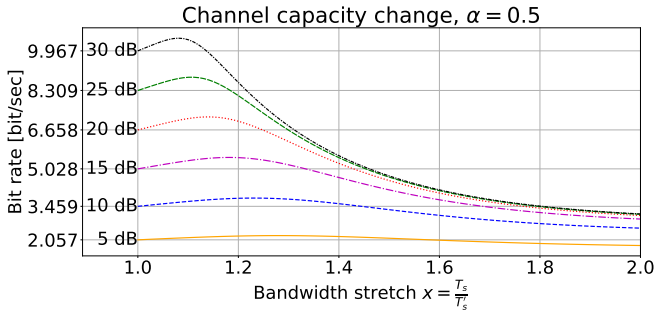

Fig. 5. The effect of the bandwidth stretch on the achievable bit rate. The channels are stretched between a factor of 1 and 2. The roll-off factor is $\alpha = 0.5$.

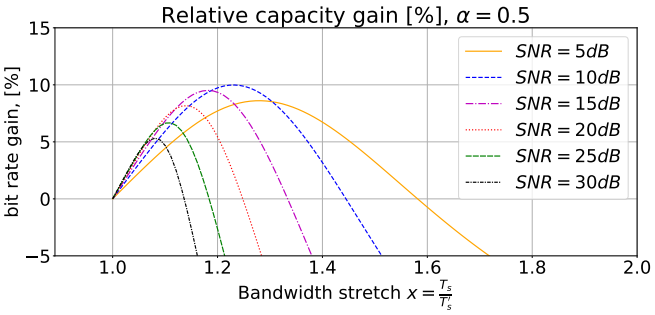

Fig. 6. The relative gain of bit rate (in %) depending on the stretching factor, and the initial SNR. The channels are stretched between a factor of 1 and 2. The roll-off factor is $\alpha = 0.5$.

With these notations, we can express the increase in noise level caused by interference from a single side, as described in [14], as:

$$\frac{N_0'}{N_0} = SNR_2 \frac{N^e}{T_{s_2}} \tag{18}$$

Here, SNR_2 and T_{s_2} represent the original (pre-stretching) signal-to-noise ratio and signaling period of the overlapping neighbor.

We have neighbors from both sides (one from the left, one from the right) with independent interference, so we have to add the equivalent noise from both. If the neighbors' signals have the same spectral shape and the same power level (same SNR), the noise is simply doubled. However, if the power level of the neighboring signals differs, let's denote the SNR levels as SNR_{2_L} and SNR_{2_R}, $SNR_{2_S} = SNR_{2_L} + SNR_{2_R}$, we have to account for both noise contributions:

$$\frac{N_{02}'}{N_0} = (SNR_{2_L} + SNR_{2_R}) \frac{N^e}{T_s} \tag{19}$$

$$= SNR_{2_S} \frac{N^e}{T_s} \tag{20}$$

where N_{02}' represents the equivalent noise power resulting from both neighbors.

If other signal parameters also differ, we have to evaluate 17 and 18 separately for the two neighbors and then add the results together.

The achievable rate for the channel is:

$$C_1 = x \cdot W_1 \cdot \log_2 \left(1 + \frac{P_1}{x \cdot W_1 \cdot N_0 \cdot \left(1 + \frac{N_{02}'}{N_0}\right)} \right)$$

$$= \frac{x}{T_{s_1}} \cdot \log_2 \left(1 + \frac{SNR_1}{x} \frac{1}{\left(1 + SNR_{2_S} \frac{N^e}{T_{s_2}}\right)} \right) \tag{21}$$

IV. Evaluation of the System Capacity

We can evaluate (21) depending on the stretching factor x for different values of the system parameters T_{s_1}, T_{s_2}, α_1, α_2, and the receiving conditions SNR_1 and SNR_2. Since our initial model is based on massive machine-type communication applications, we suppose that there are a lot of independent channels side by side with the same (or at least similar) parameters. So, in the following evaluation, we will assume that the signaling time ($T_{s_1} = T_{s_2} = T_s$) and the roll-off factor ($\alpha_1 = \alpha_2 = \alpha$) of the neighboring channels are the same. We also assume that all the channels are using the same bandwidth stretching strategy, so the channel in question have interference from both sides the same way.

For the shake of simplicity, at first we will also assume that the SNR conditions are the same for the neighboring channels. This is a feasible assumption in downlink communication when a base station is broadcasting signals to many client stations: the clients may have different channels to the base station, but a given client receives their own signal and the neighboring channels through the same channel. For uplink communication, when many clients are transmitting to a base station from possible different locations, the channel conditions may differ from channel to channel. Later we will investigate the effect of the neighboring channels having higher or lower power level. In the first case, the channel in question and the interfering channels have the same spectral power density, so they interfere with each other the same way. In the later case we can expect the stronger channel to effect the weaker channel more negatively, so in this case a global optimization is needed to decide the optimal stretching factor. We can go up to the stretching factor $x = \frac{T_s}{T_s'} = 2$ without the two neighboring channels from the two sides interfering with each other.

A. The Effect of Initial SNR

The initial SNR condition for our channels has a significant effect on how much capacity we can gain or lose by stretching the channels. Additionally, the actual shape of the spectral density of our signals, determined by the roll-off factor α, also impacts how much we can gain and at what stretching factor we can achieve the most. The SNR represents an environmental condition, while the value of the roll-off parameter α is a system design parameter. We will investigate the effect of both.

In figure 5, we can see the achievable bit rate according to (21). The horizontal axis represents the stretching factor, $x = \frac{T_s}{T_s'}$. The starting point of the curves, $x = 1$, corresponds to no stretching. At this point, the bit rate matches the Shannon capacity (1) of the channel at the given SNR level. We have

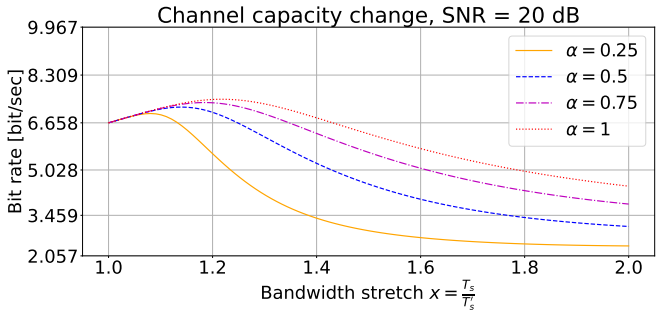

Fig. 7. The effect of the roll-off parameter on the achievable bit rate while stretching the bandwidth. The channels are stretched between a factor of 1 and 2. The initial SNR is $SNR = 20$ dB.

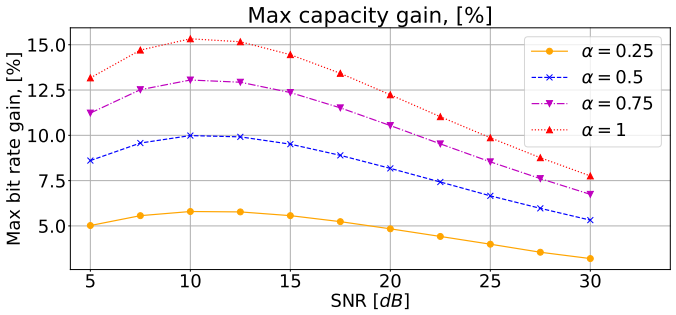

Fig. 8. The maximum achievable capacity gain while stretching the bandwidth for different initial SNR. This optimum capacity gain is achieved at different stretching factors.

chosen $\alpha = 0.5$ for this investigation; we will discuss the effect of the α parameter later.

The most significant observation in the figure is that at low stretching factor values, we can increase capacity at any SNR level. When the initial channel condition is good, with a high SNR, the maximum gain is achieved at a low stretching level. Conversely, when the initial channel condition is worse, with a low SNR, we need to stretch more to reach the maximum capacity gain. However, regardless of the SNR condition, there is a level of stretching that is excessive, causing a decrease in capacity.

The amount of maximal capacity gain is higher at higher SNR conditions, but the base capacity level (corresponding to $x = 1$) is also higher. In figure 6, we can observe the bit rate gain in percentage relative to the base capacity. Here, 0 represents the starting level, with positive values indicating capacity gain and negative values indicating capacity loss. For different SNR conditions, there is a distinct, optimal stretching factor at which we can achieve the most significant gains.

B. The Effect of Roll-off Factor

The achievable capacity gain also depends on the channel filter characteristics, specifically the roll-off factor, α. When the channel filter is steep (the α value is small), even a slight amount of stretching results in a significant overlap between neighboring channels, causing excess noise to increase rapidly. In this scenario, it also implies that the original system's channel usage was close to the Nyquist limit, indicating that the original signaling scheme was already bandwidth-efficient.

Conversely, when the channel filter is shallow (corresponding to larger α values), stretching leads to overlap in the portion of the spectral density function that is small. This results in minor interference and minimal excess noise. In such cases, we anticipate gaining much more capacity by extending the bandwidth than what we lose due to excess noise.

In figure 7, we can observe the change in channel capacity versus the stretching factor for various roll-off factors. The initial SNR is chosen to be 20 dB. Two key observations emerge: Firstly, the maximum achievable channel capacity is lower for lower α values (steep channel filter). Secondly, it is evident that the maximum channel capacity is reached at a lower stretching factor. Beyond this point, any further increase in the stretching factor results in a loss of capacity.

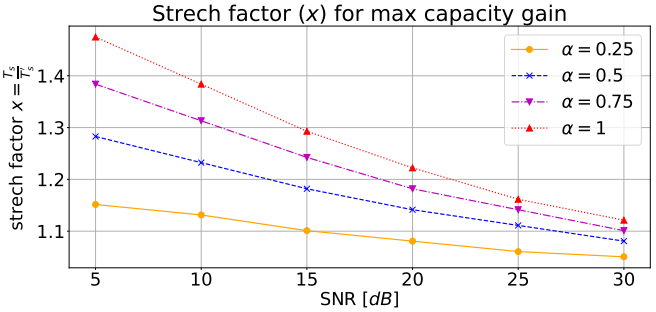

Fig. 9. The dependence of optimal stretching factor, at which the maximal bit rate gain is achieved, on the initial SNR.

C. The Maximum Achievable Capacity Gain

For every combination of parameters, both the environmental parameter SNR and the design parameter α, there exists an optimal stretching factor by which we can achieve the highest capacity. In figure 8, we can observe the maximum capacity gain, expressed as a percentage of the base capacity, versus the initial SNR for four different α values. It's important to note that this maximum capacity is not achieved at the same stretching level. Instead, for every point on the graph, there is a corresponding optimal stretching factor. Around this optimal stretching factor, capacity gains are attainable for every combination of SNR conditions and α values. The higher the roll-off factor (α) used, the more we can gain by stretching. For $\alpha = 0.25$, about a 5% capacity gain can be achieved, and it is less dependent on the channel condition. When a shallower roll-off (higher α value) is used, the achievable capacity gain is around 10-15%, and it is highly dependent on the SNR condition.

This optimal stretching factor value can be observed in figure 9. As expected, for shallower roll-off (higher α value), a higher optimal stretching factor is needed. Additionally, we can observe that for a given α parameter, the lower the SNR, the more stretching is required.

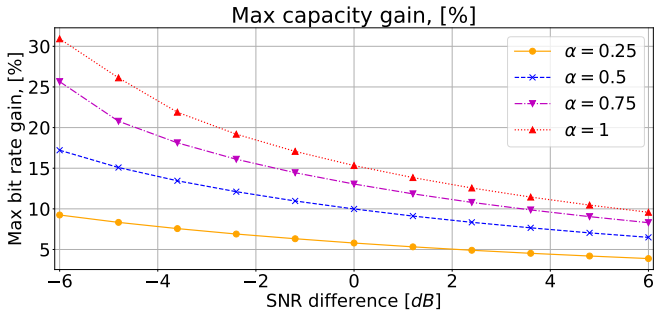

Fig. 10. The maximum achievable capacity gain as a function of the power level difference of neighboring channels compared to the current channel. Negative values indicate that the neighbors are weaker, while positive values indicate that the neighbors are stronger. For the sake of clarity, we assume that both neighbors have the same higher or lower SNR level.

D. Different Power Level in Neighboring Channels

The assumption that the power level of the neighboring channels' signals is the same is not always feasible. One practically important case is uplink communication, where the transmitting client stations may be at different distances from the base station, resulting in different received power levels at the base station, even if the client stations are transmitting at the same nominal power level.

When the power levels of the neighboring channels are different, the situation is no longer symmetrical regarding the interference the overlapping signals cause to each other. In figure 10, we can investigate the maximum achievable capacity gain when the neighboring channels have higher or lower power levels. As expected, when the neighbors' SNR is lower compared to the SNR of the current channel, the interference caused by the overlap is lower, resulting in a higher capacity gain. Conversely, in the neighboring channel, the stronger signal causes more interference, leading to a lower capacity gain. However, the figure shows that even when the neighbors have an SNR level 6 dB higher (four times higher power level) from both sides, capacity can still be gained by allowing overlapping.

This scenario presents an opportunity for resource allocation optimization, depending on the needs of the individual channels.

V. Conclusions

In this paper, we have proposed a solution to enhance the utilization of available bandwidth in a multi-user environment employing frequency division multiple access (FDMA). Our proposed method relaxes the orthogonality requirement of the classic FDMA scheme, permitting a partial overlap between neighboring channels. However, it's important to note that we do not fully adopt power domain NOMA schemes; we retain distinct frequency channels and do not propose the implementation of successive interference cancellation (SIC) to maintain the simplicity of the receiver implementation.

Our approach focuses on expanding the frequency bands of individual channels, allowing them to partially overlap with neighboring channels, potentially increasing channel capacity. We have demonstrated that by applying the right amount of stretching this capacity increase surpasses the capacity loss attributed to interference caused by the overlap.

Through numerical calculations, we have determined the optimal degree of frequency band stretching, which depends on the spectral characteristics of the signals in use and the signal-to-noise ratio (SNR) conditions of the channels. Our findings consistently reveal capacity improvements ranging from 5% to 15% across all examined cases. The optimal stretching level can be determined based on the channel conditions. Notably, we have found that a larger roll-off factor (α parameter) in the channel filter, indicative of a shallower filter characteristic, permits more extensive stretching and results in more significant capacity gains.

First, we conducted our numerical calculations on the case where all channels have the same parameters. However, the derived formulas also apply to cases where the channels have different parameters (such as signaling rate or roll-off) or SNR conditions. Later, we extended our studies to scenarios with varying SNR conditions in uplink communication. We concluded that when neighboring channels have different SNR conditions (different receive power levels), the stronger channel can gain more capacity, but the weaker channel can also achieve a capacity gain. Further study could extend to investigating optimal resource allocation based on individual channel needs.

The proposed method does not directly compete with systems applying full NOMA with SIC; depending on the channel conditions, one or the other may perform better. In situations where the SNR conditions of the overlapping channels are similar, SIC cannot gain capacity, while the proposed method works best in this scenario. One important aspect of the proposed method (as opposed to full NOMA with SIC) is that it does not increase receiver complexity, and traditional FDMA systems can be easily extended to implement this method.

References

[1] Y. Liu, Z. Qin, M. Elkashlan, Z. Ding, A. Nallanathan, and L. Hanzo, "Nonorthogonal Multiple Access for 5G and Beyond," *Proceedings of the IEEE*, vol. 105, no. 12, pp. 2347–2381, 2017, doi: https://doi.org/10.1109/JPROC.2017.2768666.

[2] L. Dai, B. Wang, Y. Yuan, S. Han, I. Chih-Lin, and Z. Wang, "Non-orthogonal multiple access for 5g: solutions, challenges, opportunities, and future research trends," *IEEE Communications Magazine*, vol. 53, no. 9, pp. 74–81, 2015, doi: https://doi.org/10.1109/MCOM.2015.7263349.

[3] L. Dai, B. Wang, Z. Ding, Z. Wang, S. Chen, and L. Hanzo, "A survey of non-orthogonal multiple access for 5g," *IEEE communications surveys & tutorials*, vol. 20, no. 3, pp. 2294–2323, 2018, doi: https://doi.org/10.1109/COMST.2018.2835558.

[4] K. Higuchi and A. Benjebbour, "Non-orthogonal multiple access (noma) with successive interference cancellation for future radio access," *IEICE Transactions on Communications*, vol. 98, no. 3, pp. 403–414, 2015, doi: https://doi.org/10.1587/transcom.E98.B.403.

[5] Y. Saito, Y. Kishiyama, A. Benjebbour, T. Nakamura, A. Li, and K. Higuchi, "Non-orthogonal multiple access (noma) for cellular future radio access," in *2013 IEEE 77th vehicular technology conference (VTC Spring)*. IEEE, 2013, pp. 1–5, doi: https://doi.org/10.1109/VTCSpring.2013.6692652.

[6] Y. Tan, J. Zhou, and J. Qin, "Novel channel estimation for non-orthogonal multiple access systems," *IEEE Signal Processing Letters*, vol. 23, no. 12, pp. 1781–1785, 2016, doi: https://doi.org/10.1109/LSP.2016.2617897.

[7] Y. Du, B. Dong, W. Zhu, P. Gao, Z. Chen, X. Wang, and J. Fang, "Joint channel estimation and multiuser detection for uplink grant-free noma," *IEEE Wireless Communications Letters*, vol. 7, no. 4, pp. 682–685, 2018, doi: https://doi.org/10.1109/LWC.2018.2810278.
[8] B. Makki, K. Chitti, A. Behravan, and M.-S. Alouini, "A survey of noma: Current status and open research challenges," *IEEE Open Journal of the Communications Society*, vol. 1, pp. 179–189, 2020.
[9] B. Kim, Y. Park, and D. Hong, "Partial non-orthogonal multiple access (p-noma)," *IEEE Wireless Communications Letters*, vol. 8, no. 5, pp. 1377–1380, 2019, doi: https://doi.org/10.1109/10.1109/LWC.2019.29187800.
[10] K. S. Ali, E. Hossain, and M. J. Hossain, "Partial non-orthogonal multiple access (noma) in downlink poisson networks," *IEEE Transactions on Wireless Communications*, vol. 19, no. 11, pp. 7637–7652, 2020, doi: https://doi.org/10.1109/TWC.2020.3014625.
[11] M. Waseem, A. Mahmood, and M. Gidlund, "Partial noma for semi-integrated sensing and communication," in *2023 IEEE Globecom Conference*, 12 2023.
[12] H. Mathur and T. Deepa, "A novel precoded digitized ofdm based noma system for future wireless communication," *Optik*, vol. 259, p. 168948, 2022. [Online]. Available: https://www.sciencedirect.com/science/article/pii/S003040262200328X
[13] J. Guerreiro, R. Dinis, P. Montezuma, and M. Campos, "On the receiver design for nonlinear noma-ofdm systems," in *2020 IEEE 91st Vehicular Technology Conference (VTC2020-Spring)*, 2020, pp. 1–6.
[14] Z. Belső and L. Pap, "Capacity analysis of partially overlapping noma system with two users," *1st Workshop on Intelligent Infocommunication Networks, Systems and Services*, pp. 47–51, 2023, doi: https://doi.org/10.1109/10.1109/10.3311/WINS2023-009.
[15] D. Tse and P. Viswanath, *Fundamentals of wireless communication*. Cambridge university press, 2005, doi: https://doi.org/10.1017/CBO9780511807213.
[16] T. M. Cover and J. A. Thomas, "Information theory and statistics," *Elements of information theory*, vol. 1, no. 1, pp. 279–335, 1991, doi: https://doi.org/10.1002/047174882X.
[17] J. Proakis and M. Salehi, *Digital Communications*. McGraw-Hill Education, 2008.
[18] A. Mraz and L. Pap, "General interference analysis of m-qam and m-psk wireless communications," *Wireless Networks*, vol. 19, pp. 331–344, 2013, doi: https://doi.org/10.1007/s11276-012-0469-5.
[19] A. Mraz, *Modeling and Optimization of Advanced Wireless Networks*. LAP LAMBERT Academic Publishing, 2013.

Zoltán Belső graduates from the Eötvös Loránd University, Faculty of Science as a Computer Scientist (M.S. degree) in 1995. He also graduated as an Electrical Engineer (M.S. degree) from the Technical University of Budapest, Faculty of Electrical Engineering, Branch of Telecommunications in 2007. He is working at the Technical University of Budapest, Faculty of Electrical Engineering, Department of Telecommunications since graduated there as a part time lecturer. He has worked on Unmanned Aerial Vehicle (UAV) communications systems and Quantum Key Distribution Systems (QKD).

László Pap graduated from the Technical University of Budapest, Faculty of Electrical Engineering, Branch of Telecommunications. He became Dr. Univ. and Ph.D. in 1980, and Doctor of Sciences in 1992. In 2001 and 2007 he has been elected as a Correspondent and Full Member of the Hungarian Academy of Sciences. His main fields of the research are the electronic systems, nonlinear circuits, synchronization systems, modulation and coding, spread spectrum systems, CDMA, multiuser detection and mobile communication systems. His main education activity has covered the fields of electronics, modern modulation and coding systems, communication theory, introduction to mobile communication. Professor Pap had been Head of the Dept. of Telecommunications, the Dean of the Faculty of Electrical Engineering at Budapest University of Technology and Economics, and Vice Rector of the University.